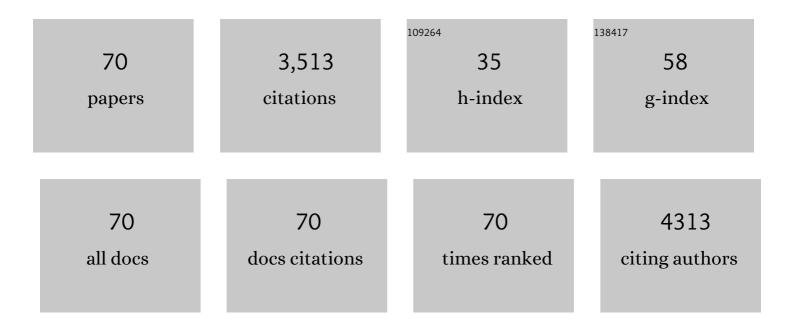


## List of Publications by Year in descending order

Source: https://exaly.com/author-pdf/101808/publications.pdf Version: 2024-02-01



Ιτιν Ρανι

#	Article	IF	CITATIONS
1	Photocorrosion inhibition and high-efficiency photoactivity of porous g-C3N4/Ag2CrO4 composites by simple microemulsion-assisted co-precipitation method. Applied Catalysis B: Environmental, 2017, 204, 78-88.	10.8	170
2	CTAB-assisted synthesis of novel ultrathin MoSe <sub>2</sub> nanosheets perpendicular to graphene for the adsorption and photodegradation of organic dyes under visible light. Nanoscale, 2016, 8, 440-450.	2.8	163
3	Unveiling Role of Sulfate Ion in Nickelâ€Iron (oxy)Hydroxide with Enhanced Oxygenâ€Evolving Performance. Advanced Functional Materials, 2021, 31, 2102772.	7.8	158
4	Hierarchical flower-like SnSe2 supported Ag3PO4 nanoparticles: Towards visible light driven photocatalyst with enhanced performance. Applied Catalysis B: Environmental, 2017, 202, 326-334.	10.8	154
5	Enhanced performance of doped BiOCl nanoplates for photocatalysis: understanding from doping insight into improved spatial carrier separation. Journal of Materials Chemistry A, 2017, 5, 12542-12549.	5.2	138
6	In situ construction of an SnO <sub>2</sub> /g-C <sub>3</sub> N <sub>4</sub> heterojunction for enhanced visible-light photocatalytic activity. RSC Advances, 2015, 5, 68953-68963.	1.7	123
7	Insights into the synergy effect of anisotropic {001} and {230}facets of BaTiO3 nanocubes sensitized with CdSe quantum dots for photocatalytic water reduction. Applied Catalysis B: Environmental, 2018, 227, 1-12.	10.8	116
8	Construction of Z-Scheme System for Enhanced Photocatalytic H <sub>2</sub> Evolution Based on CdS Quantum Dots/CeO <sub>2</sub> Nanorods Heterojunction. ACS Sustainable Chemistry and Engineering, 2018, 6, 2552-2562.	3.2	105
9	Constructing 2D BiOCl/C3N4 layered composite with large contact surface for visible-light-driven photocatalytic degradation. Applied Surface Science, 2017, 426, 897-905.	3.1	95
10	Rational Design of Z-Scheme System Based on 3D Hierarchical CdS Supported 0D Co <sub>9</sub> S <sub>8</sub> Nanoparticles for Superior Photocatalytic H <sub>2</sub> Generation. ACS Sustainable Chemistry and Engineering, 2018, 6, 10385-10394.	3.2	95
11	A green and facile strategy for preparation of novel and stable Cr-doped SrTiO3/g-C3N4 hybrid nanocomposites with enhanced visible light photocatalytic activity. Journal of Alloys and Compounds, 2015, 647, 456-462.	2.8	91
12	Constructing a direct Z-scheme photocatalytic system based on 2D/2D WO <sub>3</sub> /ZnIn <sub>2</sub> 4 nanocomposite for efficient hydrogen evolution under visible light. Inorganic Chemistry Frontiers, 2019, 6, 929-939.	3.0	88
13	Dynamic dissolution and re-adsorption of molybdate ion in iron incorporated nickel-molybdenum oxyhydroxide for promoting oxygen evolution reaction. Applied Catalysis B: Environmental, 2022, 307, 121150.	10.8	88
14	Layered-Structure SbPO <sub>4</sub> /Reduced Graphene Oxide: An Advanced Anode Material for Sodium Ion Batteries. ACS Nano, 2018, 12, 12869-12878.	7.3	87
15	SnP <sub>2</sub> O <sub>7</sub> Covered Carbon Nanosheets as a Longâ€Life and Highâ€Rate Anode Material for Sodiumâ€Ion Batteries. Advanced Functional Materials, 2018, 28, 1804672.	7.8	84
16	lron-nitrogen-carbon species for oxygen electro-reduction and Zn-air battery: Surface engineering and experimental probe into active sites. Applied Catalysis B: Environmental, 2019, 254, 601-611.	10.8	78
17	Facile fabrication of novel porous graphitic carbon nitride/copper sulfide nanocomposites with enhanced visible light driven photocatalytic performance. Journal of Colloid and Interface Science, 2016, 476, 132-143.	5.0	74
18	Manganese oxide at cadmium sulfide (MnOx@CdS) shells encapsulated with graphene: A spatially separated photocatalytic system towards superior hydrogen evolution. Journal of Colloid and Interface Science, 2019, 533, 452-462.	5.0	72

Jun Pan

#	Article	IF	CITATIONS
19	Achieving electronic structure reconfiguration in metallic carbides for robust electrochemical water splitting. Journal of Materials Chemistry A, 2020, 8, 2453-2462.	5.2	71
20	Compositionâ€Tunable Vertically Aligned CdS <sub><i>x</i></sub> Se <sub>1â€<i>x</i></sub> Nanowire Arrays via van der Waals Epitaxy: Investigation of Optical Properties and Photocatalytic Behavior. Advanced Materials, 2012, 24, 4151-4156.	11.1	69
21	Facet and morphology dependent photocatalytic hydrogen evolution with CdS nanoflowers using a novel mixed solvothermal strategy. Journal of Colloid and Interface Science, 2018, 513, 222-230.	5.0	62
22	One-Dimensional SnO <sub><b>2</b></sub> Nanostructures: Synthesis and Applications. Journal of Nanotechnology, 2012, 2012, 1-12.	1.5	60
23	Self-integrated β-Bi2O3/Bi2O2.33@Bi2O2CO3 ternary composites: Formation mechanism and visible light photocatalytic activity. Applied Surface Science, 2018, 430, 613-624.	3.1	60
24	Phase Transformation Synthesis of Strontium Tantalum Oxynitride-Based Heterojunction for Improved Visible Light-Driven Hydrogen Evolution. ACS Applied Materials & Interfaces, 2018, 10, 21328-21334.	4.0	55
25	Simple and facile ultrasound-assisted fabrication of Bi2O2CO3/g-C3N4 composites with excellent photoactivity. Journal of Colloid and Interface Science, 2017, 497, 144-154.	5.0	53
26	C–S bond induced ultrafine SnS <sub>2</sub> dot/porous g-C <sub>3</sub> N <sub>4</sub> sheet 0D/2D heterojunction: synthesis and photocatalytic mechanism investigation. Dalton Transactions, 2017, 46, 17032-17040.	1.6	50
27	Enhanced visible-light photocatalytic degradation by Mn <sub>3</sub> O <sub>4</sub> /CeO <sub>2</sub> heterojunction: a Z-scheme system photocatalyst. Inorganic Chemistry Frontiers, 2018, 5, 2579-2586.	3.0	50
28	Rational design and preparation of few-layered MoSe <sub>2</sub> nanosheet@C/TiO <sub>2</sub> nanobelt heterostructures with superior lithium storage performance. RSC Advances, 2016, 6, 23161-23168.	1.7	47
29	Synergetic utilization of photoabsorption and surface facet in crystalline/amorphous contacted BiOCI-Bi2S3 composite for photocatalytic degradation. Journal of Alloys and Compounds, 2019, 780, 907-916.	2.8	46
30	Prussian blue analogue-derived Mn–Fe oxide nanocubes with controllable crystal structure and crystallinity as highly efficient OER electrocatalysts. Journal of Alloys and Compounds, 2020, 820, 153438.	2.8	45
31	Copper–nickel embedded into a nitrogen-doped carbon octahedron as an effective bifunctional electrocatalyst. Inorganic Chemistry Frontiers, 2018, 5, 2276-2283.	3.0	42
32	Interfaces of graphitic carbon nitride-based composite photocatalysts. Inorganic Chemistry Frontiers, 2020, 7, 4754-4793.	3.0	41
33	Interface engineering in CeO2 (1 1 1) facets decorated with CdSe quantum dots for photocatalytic hydrogen evolution. Journal of Colloid and Interface Science, 2020, 579, 707-713.	5.0	41
34	Voltage-Modulated Structure Stress for Enhanced Electrochemcial Performances: The Case of μ-Sn in Sodium-Ion Batteries. Nano Letters, 2021, 21, 3588-3595.	4.5	38
35	Boosting charge transfer via molybdenum doping and electric-field effect in bismuth tungstate: Density function theory calculation and potential applications. Journal of Colloid and Interface Science, 2019, 534, 20-30.	5.0	36
36	Effect of sodium doping on the structure and enhanced photocatalytic hydrogen evolution performance of graphitic carbon nitride. Molecular Catalysis, 2017, 433, 128-135.	1.0	35

Jun Pan

#	Article	IF	CITATIONS
37	Intimate contacted two-dimensional/zero-dimensional composite of bismuth titanate nanosheets supported ultrafine bismuth oxychloride nanoparticles for enhanced antibiotic residue degradation. Journal of Colloid and Interface Science, 2018, 529, 23-33.	5.0	35
38	Fabrication of bismuth titanate nanosheets with tunable crystal facets for photocatalytic degradation of antibiotic. Journal of Materials Science, 2019, 54, 13740-13752.	1.7	35
39	Insight into the amorphous nickel-iron (oxy)hydroxide catalyst for efficient oxygen evolution reaction. Journal of Colloid and Interface Science, 2021, 591, 307-313.	5.0	34
40	Multiple active components, synergistically driven cobalt and nitrogen Co-doped porous carbon as high-performance oxygen reduction electrocatalyst. Inorganic Chemistry Frontiers, 2017, 4, 1748-1756.	3.0	32
41	Insights into the efficient charge separation and transfer efficiency of La,Cr-codoped SrTiO <sub>3</sub> modified with CoP as a noble-metal-free co-catalyst for superior visible-light driven photocatalytic hydrogen generation. Inorganic Chemistry Frontiers, 2018, 5, 679-686.	3.0	31
42	Self-assemble SnO <sub>2</sub> @TiO <sub>2</sub> porous nanowire–nanosheet heterostructures for enhanced photocatalytic property. CrystEngComm, 2014, 16, 10863-10869.	1.3	29
43	In situ formation of carbon encapsulated nanosheet-assembled MoSe2 hollow nanospheres with boosting lithium storage. Journal of Colloid and Interface Science, 2017, 491, 279-285.	5.0	29
44	Sulphur and nitrogen dual-doped mesoporous carbon hybrid coupling with graphite coated cobalt and cobalt sulfide nanoparticles: Rational synthesis and advanced multifunctional electrochemical properties. Journal of Colloid and Interface Science, 2018, 509, 254-264.	5.0	29
45	Construction of two dimensional Sr2Ta2O7/S-doped g-C3N4 nanocomposites with Pt cocatalyst for enhanced visible light photocatalytic performance. Applied Surface Science, 2019, 478, 334-340.	3.1	28
46	Well-organized migration of electrons for enhanced hydrogen evolution: Integration of 2D MoS2 nanosheets with plasmonic photocatalyst by a facile ultrasonic chemical method. Journal of Colloid and Interface Science, 2017, 508, 559-566.	5.0	27
47	Boosted electrocatalytic activity of nitrogen-doped porous carbon triggered by oxygen functional groups. Journal of Colloid and Interface Science, 2019, 541, 133-142.	5.0	23
48	Ultrafast interfacial charge evolution of the Type-II cadmium Sulfide/Molybdenum disulfide heterostructure for photocatalytic hydrogen production. Journal of Colloid and Interface Science, 2022, 619, 246-256.	5.0	23
49	Crystalline Sb or Bi in amorphous Ti-based oxides as anode materials for sodium storage. Chemical Engineering Journal, 2020, 380, 122624.	6.6	22
50	Shape-dependent hydrogen generation performance of PtPd bimetallic co-catalyst coupled with C3N4 photocatalyst. Rare Metals, 2021, 40, 3554-3560.	3.6	20
51	One-pot nitridation route synthesis of SrTaO2N/Ta3N5 type II heterostructure with enhanced visible-light photocatalytic activity. Journal of Colloid and Interface Science, 2019, 554, 74-79.	5.0	19
52	Improved photocatalytic hydrogen evolution by facet engineering of core-shell structural CdS@ZnO. International Journal of Hydrogen Energy, 2019, 44, 25599-25606.	3.8	17
53	A Novel Metal–Organic Framework Intermediated Synthesis of Heterogeneous CoS <sub>2</sub> /CoS Porous Nanosheets for Enhanced Oxygen Evolution Reaction. Energy Technology, 2021, 9, 2000961.	1.8	17
54	Novel two-dimensional Bi <sub>4</sub> V <sub>2</sub> O <sub>11</sub> nanosheets: controllable synthesis, characterization and insight into the band structure. CrystEngComm, 2018, 20, 1116-1122.	1.3	16

Jun Pan

#	Article	IF	CITATIONS
55	Efficient hydrogen generation of indium doped BaTiO3 decorated with CdSe quantum dots: Novel understanding of the effect of doping strategy. International Journal of Hydrogen Energy, 2019, 44, 1627-1639.	3.8	16
56	One-step chemical bath co-precipitation method to prepare high hydrogen-producing active ZnxCd1-xS solid solution with adjustable band structure. Journal of Materials Science, 2021, 56, 5717-5729.	1.7	14
57	Abundant hydroxyl groups decorated on nitrogen vacancy-embedded g-C <sub>3</sub> N <sub>4</sub> with efficient photocatalytic hydrogen evolution performance. Catalysis Science and Technology, 2021, 11, 3914-3924.	2.1	14
58	Ion-biosorption induced core–shell Fe <sub>2</sub> P@carbon nanoparticles decorated on N, P co-doped carbon materials for the oxygen evolution reaction. Inorganic Chemistry Frontiers, 2021, 8, 2385-2394.	3.0	14
59	Investigating the active sites in molybdenum anchored nitrogen-doped carbon for alkaline oxygen evolution reaction. Journal of Colloid and Interface Science, 2022, 609, 617-626.	5.0	14
60	Metal–organic framework-driven copper/carbon polyhedron: synthesis, characterization and the role of copper in electrochemistry properties. Journal of Materials Science, 2018, 53, 7755-7766.	1.7	13
61	BODIPY modified g-C3N4 as a highly efficient photocatalyst for degradation of Rhodamine B under visible light irradiation. Journal of Solid State Chemistry, 2018, 267, 22-27.	1.4	13
62	Controlled preparation of hollow Zn0.3Cd0.7S nanospheres modified by NiS1.97 nanosheets for superior photocatalytic hydrogen production. Journal of Colloid and Interface Science, 2022, 606, 1-9.	5.0	13
63	Construction of S-scheme BiOCl/CdS composite for enhanced photocatalytic degradation of antibiotic. Journal of Materials Science: Materials in Electronics, 2022, 33, 13303-13315.	1.1	13
64	Highly efficient adsorption/photodegradation of organic pollutants using Sn1â^0.25xCuxS2 flower-like as a novel photocatalyst. Journal of Alloys and Compounds, 2017, 702, 489-498.	2.8	9
65	Electrostatic self-assembly of 2D/2D Bi2WO6/ZnIn2S4 heterojunction with enhanced photocatalytic degradation of tetracycline hydrochloride. Journal of Solid State Chemistry, 2022, 314, 123408.	1.4	9
66	Sodium borohydride-assisted synthesis of strontium substituted lanthanum cobaltate with in-situ generated cobaltosic oxide: Towards enhanced oxygen evolution reaction in alkaline media. Journal of Colloid and Interface Science, 2019, 557, 103-111.	5.0	8
67	In situ synthesis of cubic PtPd bimetallic co-catalyst on C3N4 nanosheets for photocatalytic hydrogen generation. Journal of Nanoparticle Research, 2021, 23, 1.	0.8	6
68	Ru-optimized geometric sites of cations in CoFe/CoFe2O4 electrocatalysts with graphitic carbon shells for boosting water oxidation. Electrochimica Acta, 2022, 425, 140665.	2.6	6
69	The Inâ€situ Growth of Ru Modified CoP Nanoflakes on Carbon Clothes as Efficient Electrocatalysts for HER**. ChemElectroChem, 2022, 9, .	1.7	3
70	Rational design of 0D/3D Sn <sub>3</sub> O <sub>4</sub> /NiS nanocomposites for enhanced photocatalytic hydrogen generation. New Journal of Chemistry, 2022, 46, 14043-14051.	1.4	2